

TEMPERATURE DEPENDENCE OF THE FIRST ORDER RAMAN SCATTERING IN THIN FILMS OF $\mu\text{c-Si:H}$

M. F. Cerqueira*, J. A. Ferreira
Dep^{to} de Física, Universidade do Minho- 4709 Braga- Portugal

*to whom all correspondence should be send

Abstract: The temperature effect on microcrystalline silicon ($\mu\text{c-Si:H}$) films produced by R.F. magnetron sputtering has been studied by Raman spectroscopy. The thermal behaviour of $\mu\text{c-Si:H}$ films and crystalline silicon is compared and interpreted on the basis of anharmonic effects.

We have studied the first order Raman spectra of our films for several Ar^+ laser powers. Our results show a blue shift and a broadening of the Raman spectra with increasing the laser power. This effect is not due to structural changes since it is reproducible.

The sample temperature has been calculated according to the well known relation between Stokes and anti-Stokes components.

Our results show that the temperature effect is stronger in $\mu\text{c-Si:H}$ than in crystalline silicon. This difference can be attributed to the size of the microcrystals, which are imbedded in a amorphous matrix surrounded by a third phase called grain boundary.

Keywords: Microcrystalline silicon, anharmonic effects, Raman scattering

1. Introduction

Hydrogenated microcrystalline silicon ($\mu\text{c-Si:H}$) has attracted considerable attention as a potential new material for electronic devices such as solar cells, thin films transistors and MOSFETs. This interest is based on a higher electrical conductivity of this material compared to amorphous silicon (a-Si:H). Nevertheless, electrical conductivity and other physical properties relevant for those applications are strongly influenced by the thin film microstructure of $\mu\text{c-Si:H}$.

Raman scattering is commonly used as a complementary technique for the structural characterization in this kind of materials. This technique is in principle a powerful technique although several experimental effects must be taken into account: i) The peak frequency of the 1st optical phonon decreases with increasing temperature owing to anharmonic effects; ii) $\mu\text{c-Si:H}$ thin films crystallise easily; and iii) thin film strain (and stress) shifts the phonon frequency.

In this paper we will study the anharmonic effects observed in this material, since they are different from those observed in crystalline silicon.

Due to the anharmonicity of the lattice forces, an optical mode can interchange energy with other lattices modes, and in this way maintain a thermal equilibrium energy content. In this respect an optical mode behaves similarly to an acoustical mode. The relaxation time of optical modes influence the linewidth of the peak observed in Raman

scattering. Lifetime is related to the linewidth through the energy-time uncertainty relation. This fact implies that the linewidth is determined by energy relaxation processes.

The main anharmonic interaction is due to the splitting of an optical phonon into two acoustic phonons of opposite momentum, that means $\omega_{q1} = \omega_{q2}$ (three phonon model^[1,2]). To describe the experimental data for bulk silicon at high temperatures it is necessary to include another contribution, the four phonon model, and $\omega_{q1} = \omega_{q2} = \omega_{q3} = \omega_0/3$ ^[3]. These phonons can belong to the same branch in the phonon dispersion curve (overtones) or to different branches (combinations). In silicon, the number of overtones is 4 and the number of combinations is 50.

In the bulk crystal of silicon is observed mainly the optical phonon in the center of the Brillouin Zone with $\omega_0 = 520 \text{ cm}^{-1}$. This is a consequence of the conservation of the momentum in crystals.

Microcrystalline silicon consists of a mixture of variable volume fractions of a crystalline phase (small crystallites), an amorphous phase and grain boundaries. The relative volume occupied by these three phases is a function of the growth conditions.

Table I: Growth conditions and thickness of two samples

sample	P (W)	pAr (Pa)	pH ₂ (Pa)	d (nm)
d10	150	0.23	0.35	1760
e11	300	0.78	0.16	518

Phonons in small crystallites are localized. Thus their momentum is no longer well defined, according to the uncertainty principle. The conservation law of the momentum is no longer strictly valid. As a consequence, all the phonons of the dispersion relation, evaluated with a weight function, contribute to the measured Raman signal. Because the phonons in the Brillouin Zone center are the ones with maximum energy, the contribution of other phonons will shift the Raman signal to lower energies accompanied by a spectral broadening.

We will present the temperature effect in two samples grown by reactive RF sputtering^[4]. One sample is microcrystalline and the other is essentially amorphous.

2. Experimental

$\mu\text{-Si:H}$ films were prepared by planar magnetron-rf-sputtering technique. A crystalline silicon wafer was used as a target (7cm diameter and 99.999 of purity). The target was sputtered by a mixture of argon and hydrogen. The growth conditions are shown in table I. The target to substrate distance was fixed at 6 cm. The system pressure during sputtering was fixed at 3.5×10^{-2} mbar. The substrate temperature was 250° C. The structure of these films was analysed by TEM, X-ray and Raman^[5]. Raman scattering experiments were performed using an Ar-laser ($\lambda = 514.5 \text{ nm}$). The laser power was varied from 0.1 to 1 W. A triple monochromator and a CCD detector complete the experimental setup.

3. Results

3.1. Raman curves

Figure 1 shows the Raman backscattering spectra of the two samples in study taken at different laser powers. As the laser power (P) is raised from 0.1 W to 1 W the peak

position of the “TO-like mode” shifts from 518 cm^{-1} to 494 cm^{-1} , with a concurrent increase of the full width at half maximum (Γ). We further observe an increase in magnitude when the laser power is increased. However the original shapes are reproduced when return to initial laser power for the same power laser.

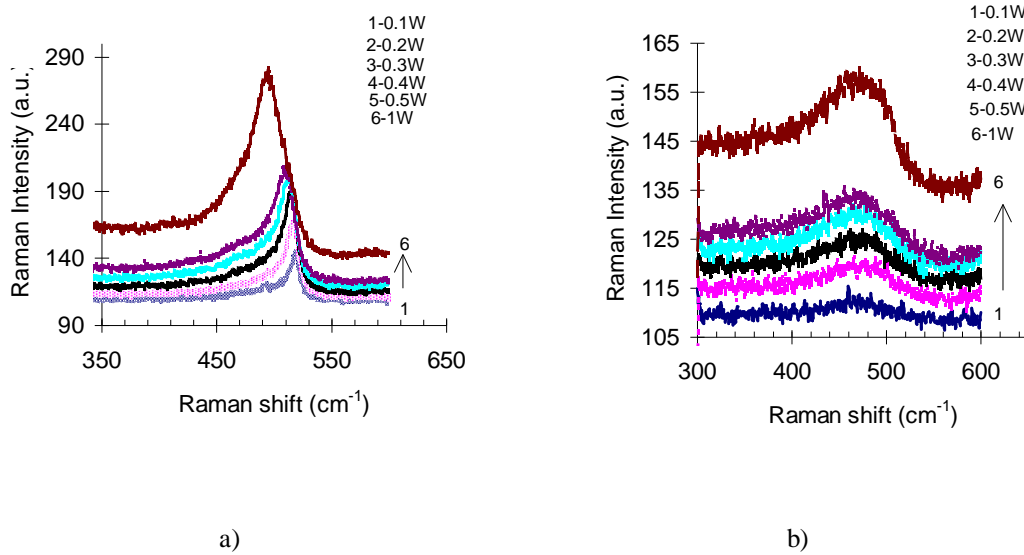


Figure 1: Raman spectra at different laser powers of a $\mu\text{c-Si:H}$ sample a) and an amorphous sample b).

Hence, we can conclude that this behavior is not due to any permanent changes in the microstructure (size, D and crystalline fraction, C).

The Raman spectra typically of these nanostructured samples shows a broad band near 480 cm^{-1} attributed to the amorphous matrix, a peak in the vicinity of 500 cm^{-1} which is related to surface modes and a peak in the vicinity of 520 cm^{-1} . This peak is generally attributed to the transverse optical mode (TO) of crystalline silicon.

To analyse the Raman spectra, we used a computer simulation, considering the spectral profile as a superposition of the amorphous spectrum and the crystalline spectrum. The crystalline profile was calculated based on the strong phonon confinement^[6,7,8,9,10] and a Gaussian profile was attributed to the amorphous TO structure and to the surface contribution.

Table II: Results of Raman scattering studies of magnetron-sputtered $\mu\text{c-Si:H}$ films

P W	ω cm^{-1}	ω_c cm^{-1}	ω_a cm^{-1}	ω_s cm^{-1}	Γ_c cm^{-1}	Γ_a cm^{-1}	Γ_s cm^{-1}
0.1	518.4	517.6	471.7	505	9.3	60	28.7
0.2	516.8	516	471.8	501.	10.3	58	23.5
				3			
0.3	514.4	514.3	471.5	500.	11.1	55.4	21.8
				5			
0.4	512	512.2	468.1	497.	12.7	57.6	22.6
				8			
0.5	508.4	510.7	468.9	499.	13.4	57.2	20.7
				3			
1	494	507.8	469	494	13.7	46	22.3

Table II summarizes the data from the Raman fitting on sample d10. Γ_c , Γ_a and Γ_s are the values of full width at half maximum of the crystalline, amorphous and surface component, respectively. The same indices are used for the peak position (ω). The crystal size and crystalline fraction calculated at 0.1 W are 69 Å and 76 %, respectively.

3.2 Temperature Determination

To determine the sample temperature, the Stokes (S) and anti-Stokes (aS) spectra at the same laser power are acquired. The temperature was calculated by the integrated ratio of these peaks. The intensity of the Stokes and anti-Stokes peaks are proportional, respectively to n_o+1 and n_o , where n_o is the thermal occupation factor. The intensity ratio is given by:

$$\frac{I_S}{I_{aS}} = \exp\left[\frac{\hbar\omega_o}{k_B T}\right] \quad (1)$$

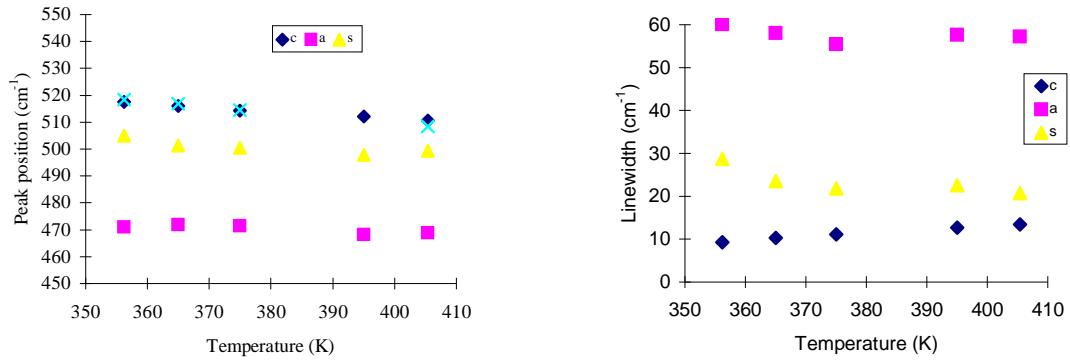
In table III the power incident on the sample is shown and the resultant sample temperatures for the laser power in study.

The heat conduction in $\mu\text{c-Si:H}$ samples is lower than in c-Si due to the presence of voids in the former. Therefore, at a given laser power the temperature in a $\mu\text{c-Si:H}$ sample is higher than in a crystalline sample.

Table III: Laser power and temperature on the sample

P (W) _{Laser}	P (mW) _{sample}	T (K) _{sample}
0.1	0.68	356
0.2	1.3	365
0.3	1.9	375
0.4	2.5	395
0.5	3.2	405
1	6.2	487

Figure 2 shows for a $\mu\text{c-Si:H}$ sample the temperature behavior of the position and full width for the 3 components presented in the spectra. Figure 3 shows the comparison between the three and four phonon models and our experimental data on sample d10 ($\mu\text{c-Si:H}$).



a) b)
 Figure 2: Temperature behavior of the position a) and linewidth b) of the crystalline – c-, amorphous -a- and surface -s- components present in the Raman spectra of a $\mu\text{-Si:H}$ sample. The crosses represent the position without deconvolution.

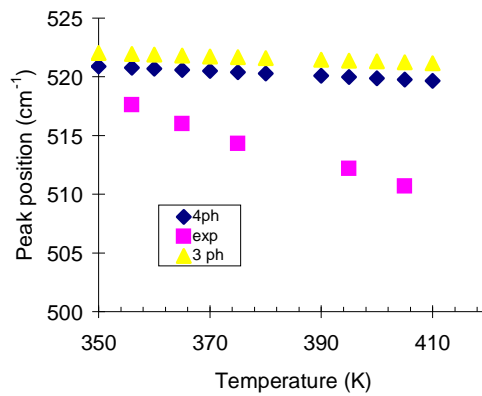


Figure 3: Temperature behavior of peak position (crystalline component) of our experimental data and the theoretical behavior assuming a three and four-phonon processes

From these figures we see that the power effect is different in the different regions, that means in the different components of the sample. The peak position of the crystalline and surface components shows the same behavior, although the linewidth behave differently. We verify that our microcrystalline samples have a temperature dependence much stronger than c-Si.

4. Conclusions

Microcrystalline material cannot be described as a single homogeneous phase, but rather as a mixture of variable volume fractions of a crystalline phase, an amorphous phase and grain boundaries (interface region between the amorphous and crystalline phases). The volume fraction occupied by the boundary phase depends on the number and also on the size of the crystallites.

The amorphous matrix of our samples shows a temperature behavior comparable to that of a-Si:H, that means no significant influence on temperature (see figure 1 b)). This is in agreement with literature.

The crystals presented in $\mu\text{-Si:H}$ thin films are finite and small. Accordingly the phonons are confined to the dimension of the crystals and as a consequence the momentum selection rule is relaxed, allowing that phonons with $q \neq 0$ could participate in the Raman process and also on the relaxation process. Then, the decay channel could not be the creation of two acoustical phonons with equal and opposite vector like in c-Si.

Since in these materials conservation of crystal momentum in the creation is relaxed and our experimental data give evidence of an increase in the decay rate of the optical phonons we believe that this relaxation is also the cause of the fast decay of the phonon modes.

The decay channel of the zone center optical mode of c-Si^[11] is the creation of two acoustical phonons of equal and opposite wavevector so that they add up to zero (due to the wavevector conservation rule). The corresponding transition probability is:

$$\Gamma_o(\omega_o) \propto |M^2| N(\omega') N(\omega'') \quad (2)$$

where M is the transition matrix element, $N(\omega)$ is the density of acoustical phonon states at energy ω and $\omega' = \omega'' = \omega_o/2 = 261 \text{ cm}^{-1}$.

Since in nanostructures the wavevector conservation rule is broken, the last equation becomes:

$$\Gamma_o(\omega_o) \propto |M|^2 \int F(\vec{q}_-, \vec{q}_+) N(\omega_o/2 - \omega') N(\omega_o/2 + \omega') d\omega' \quad (3)$$

The integration is limited to a range of energies ω' through the weighing function $F(\vec{q}_-, \vec{q}_+)$. The weighing function is given by:

$$F(\vec{q}_-, \vec{q}_+) = F\left(\left|\vec{q}\left(\omega_o/2 - \omega'\right) - \vec{q}\left(\omega_o/2 + \omega'\right)\right|\right) \quad (4)$$

and we assuming a Gaussian function of width Δq centered around $\vec{q}(\omega_o/2)$.

We expect an increase in $\Gamma(\omega_o)$ whenever the averaged two phonon density of states defined through equation (3) exceeds the two phonon density of states at $\omega_o/2$. This probability enters the temperature dependence of the Raman linewidth Γ according to^[12,13]:

$$\Gamma^2(T) = \Gamma_o^2 \left(1 + \frac{2}{e^x - 1}\right)^2 + \Gamma_1^2 \quad (5)$$

where $x = \frac{\hbar\omega_o}{2k_B T}$ and Γ_1 is the temperature independent contribution to the linewidth of microcrystals.

5. Summary

We studied the temperature effect of the Raman peak on microcrystalline thin films growth by reactive rf sputtering. We verify:

- i) The shape and position of the peak due to scattering by the Raman active mode in $\mu\text{c-Si:H}$ thin films vary for different temperatures and is reversible;
- ii) The amorphous component of the Raman peak is not sensitive to the sample temperature;
- iii) The temperature behavior of the crystalline component of $\mu\text{c-Si:H}$ samples is stronger than in bulk samples;
- iv) The behavior is not explained by 3 or 4 phonon processes;
- v) The decay channel is not the same than in c-Si owing to the relaxation of the wavevector conservation rule.

References

- [1] J. Menendez and M. Cardona, *Phys. Rev B*, 29, 2051, (1984), S. Koval and R. Migoni, *Phys. Rev B*, 49, 998, (1994)
- [2] E. Haro, M. Balkansky, R. F. Wallis and K. H. Wanser, *Phys. Rev. B* 34, 5358 (1986)
- [3] M. Balkansky, R. F. Wallis and E. Haro, *Phys. Rev. B* 28, 1928 (1983)
- [4] M. F. Cerqueira, M. Andritschky, L. Rebouta, J. A. Ferreira and M. F. Da Silva, *Vacuum vol 46 (12), p. 1385, (1995)*
- [5] M. F. Cerqueira, J. A. Ferreira, M. Andritschky and Manuel F. M. Costa, submitted to *Materials Science & Engineering B: Solid state Materials for Advanced Technology*
- [6] I. H. Campbell and P. M. Fauchet, *Solid State Commun.* 58, 739 (1986)
- [7] J. W. Ager III, D. Kveirs and G. M. Rosenblatt., *Physical Rev. B*, 43 (8), 6491 (1990)
- [8] H. Xia, Y. L. He, L. C. Wang, W. Zhang, X. K. Zhang and D. Feng, *J. Appl. Phys.* 78 (11), 6705 (1995)
- [9] Y. Kanemitsu, H. Uto et al., *Physical Rev B* 48 (4), 2827 (1993)
- [10] X. Huang, F. Ninio, L. J. Brown, S. Praver, *J. Appl. Phys.* 77 (11) (1995)
- [11] Klemens P. G., *Phys. Rev.* 148, 845, (1966)
- [12] Hart, T. R., R. L. Aggarwal and B. Lax, *Phys. Rev. B* 1, 638, (1970)
- [13] H. Richer, Z. P. Wang and L. Ley, *Solid State Commun.* 39, 625, (1981)

